

Data registration and integration of three-dimensional sensors

Baozhen Ge

Yuchen Sun

Qieni Lv

Yimo Zhang

Tianjin University

College of Precision Instrument and Opto-electronics Engineering

Key Laboratory of Opto-electronics

Information and Technical Science

Tianjin 30072, China

Abstract. Based on a vertical scanning system with a line-structured light source, data registration of several 3-D sensors is performed by a calibration process using a linear partition method. Data integration is fulfilled by using a relatively simple but efficient technique called the average coordinates method. The principle and solution procedure of each method is deduced in detail. Two 3-D sensors, a round filament target and an object with certain edge length, are used to verify the theory, and experimental results show that the mean relative error is less than 1%. With no requirement for solving nonlinear equations and other camera parameters, the method proposed is easy to adopt, runs fast, and still is high in precision, which meets the demands of 3-D measurement of a relatively big object. © 2005 Society of Photo-Optical Instrumentation Engineers. [DOI: 10.1117/1.1899405]

Subject terms: data registration; data integration; linear partition calibration; average coordinates method; 3-D sensor.

Paper 040445 received July 7, 2004; revised manuscript received Oct. 31, 2004; accepted for publication Nov. 16, 2004; published online May 11, 2005.

1 Introduction

Currently, the 3-D digitization of real objects plays a more and more important role in many fields, such as computer aided design (CAD) and computer aided manufacture (CAM), reverse engineering, rapid prototypes, virtual reality, human engineering, preservation of cultural relics, and so on.¹ Up until now, different kinds of techniques based on different principles have been proposed.² Among these techniques, noncontact optical methods, especially structured light methods have become more and more popular due to their simple principle, rapid measurement, noncontact, and high precision characteristics.

Due to the measurement range limitation of a single 3-D sensor, different techniques are adopted to obtain complete information of the object. For example, when a relatively big object is measured, such as the human body, several sensors are always placed at different positions around the object, and each of them captures part of the object.³ When a small object is measured, such as toys or models, one sensor is used and the object is placed on a rotating stage with uniform speed. Images are captured from many angles and full information is received after the stage rotates 360 deg.⁴ Therefore, data registration and integration are needed in most 3-D measurement systems, which unify the data into the same coordinates and ensures the data is complete. Many techniques are proposed for this purpose, such as the iterative closest point (ICP) method and three-points method.^{5,6} In this work, data registration and integration are performed by camera calibration using the linear partition method, which is based on a vertical scanning system with a line-structured light source.

2 Principle of Data Registration and Integration

2.1 Vertical Scanning System with Line-Structured Light Source

The vertical scanning system is based on an optical triangulation principle, as shown in Fig. 1. A line-structured light source and two black and white cameras placed at certain angles with the light source constitute the 3-D sensor, which scans vertically up and down when the object is measured. The light plane emitting from the line-structured light source intersects with the surface of the object and forms a light stripe, which can be captured by the cameras. The sensor keeps moving until the whole object is scanned by the light stripe. The horizontal plane coordinates (X_w, Y_w) are recorded by the images captured by the cameras, while the vertical coordinates Z_w are controlled by a precise mechanical scanning system, which determines the vertical resolution of the measurement. The two-camera structure can efficiently reduce or eliminate the blind areas of the cameras caused by the fluctuation on the surface.

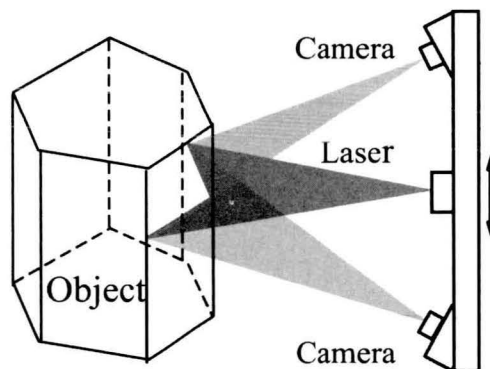


Fig. 1 Schematic diagram of a 3-D sensor.

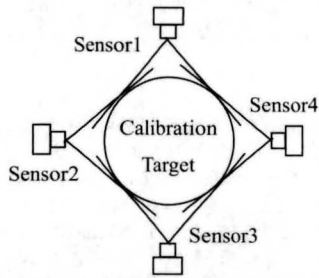


Fig. 2 Schematic diagram of multisensor calibration.

Usually, due to the measurement range limitation of a single 3-D sensor, several sensors are placed around the object and each of them can measure part of the object. The entire 3-D information will be obtained after the registration and integration of the data is received from the different sensors.

2.2 Principle of Data Registration by Camera Calibration

The mapping relationship between the space point 3-D coordinates and their corresponding image pixel coordinates can be received from camera calibration process. During the measuring process, world coordinates of the object can be calculated from the object images captured by the cameras and the calibration results. Therefore, precision of the calibration process has direct influence on the subsequent measuring process. For most of the systems with several sensors, the calibration process is always divided into two steps. The first step is called local calibration, which calibrates the sensors one by one and gets some parameters from each camera. Then, the second step, called global calibration, calibrates the translation and rotation relationship between the sensors, which fulfills the registration of the sensors. Through the analysis of the calibration process, the registration of sensors can be performed automatically if all of the sensors can be calibrated with the same calibration target and the calibration precision is high enough, as shown in Fig. 2. There are four sensors and each of them can be calibrated with part of the calibration points on the round target. Then, after the subsequent measuring process, each of the sensors will get some of the 3-D coordinates of the object, which means that the object is digitized and expressed by four sets of 3-D coordinates. Because all of the calibration points on the target are made in the same space coordinate system, these four sets of coordinates obtained by the sensors will be registered at the same space coordinate system automatically. This is the basic concept of the technique.

2.3 Calibration Target Design

The size of the calibration target will be approximately the same as the horizontal measurement range of the system, due to the data registration concept mentioned before. Therefore, the dimension of the target should be determined by special application. During the whole calibration and measurement process, each sensor has the same significance, therefore, the number and the distribution of calibra-

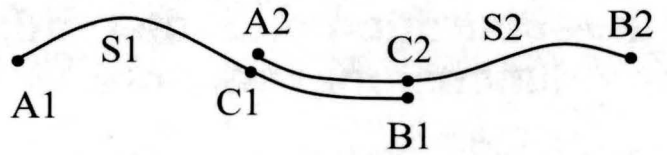


Fig. 3 Data integration of two adjacent sensors.

tion points for each sensor should be approximately identical. For most of the calibration methods, dozens of calibration points are always needed to reach a relatively high precision, which enhances the complexity of the target in return. So the design of the target and the selection of the calibration method is the key part of data registration. In this work, a round filament target and the linear partition method are adopted to calibrate the system. The target is composed of 66 steel filaments with known order and coordinates. Because the system focuses on the digitization of a relatively large object, such as the human body, the diameter of the target is about 1 m. The diameter of the filament is about 0.7 mm, and when a light plane intersects with the filaments, bright dots will formed, which can serve as coplanar calibration points during the calibration process. After the calibration process, the object to be digitized will be placed at the target position and the target will be removed. Then, the measurement process starts.

2.4 Principle of the Linear Partition Method

Many calibration techniques have been proposed, such as the direct linear transformation method, the full-scale non-linear optimization method, the two-stage method, the neural network method, and so on.^{7,8} For most of these methods, complicated camera models always need to be set up and many cameras' intrinsic and outside parameters need to be calculated, which always results in a complex and sometimes unstable solution procedure. However, in many applications, the mapping relationship between space point coordinates and their corresponding pixel coordinates in the image is enough and the camera's intrinsic and outside parameters are redundant. Based on this concept, a calibration technique with the linear partition method is proposed.

For this method, the mapping relationship between an object's space coordinates (X_w, Y_w, Z_w) and their corresponding pixel coordinates (X_f, Y_f) received from the image capture process can be formulated in matrix form with homogeneous coordinates as in following equation.

$$\rho \begin{bmatrix} X_f \\ Y_f \\ 1 \end{bmatrix} = \begin{bmatrix} m_{11} & m_{12} & m_{13} & m_{14} \\ m_{21} & m_{22} & m_{23} & m_{24} \\ m_{31} & m_{32} & m_{33} & m_{34} \end{bmatrix} \cdot \begin{bmatrix} X_w \\ Y_w \\ Z_w \\ 1 \end{bmatrix} = \mathbf{M} \cdot \begin{bmatrix} X_w \\ Y_w \\ Z_w \\ 1 \end{bmatrix}, \tag{1}$$

where ρ is a scale factor. Apparently, the matrix \mathbf{M} contains all of the mapping information, and if the number of the calibration points is enough, \mathbf{M} can be determined by solving a linear system of equations, which can be created by using calibration point 3-D coordinates and their corresponding pixel coordinates on the image. Equation (1) can be expanded as follows.

$$\begin{cases} m_{11}X_w + m_{12}Y_w + m_{13}Z_w + m_{14} - m_{31}X_f X_w - m_{32}X_f Y_w - m_{33}X_f Z_w = m_{34}X_f \\ m_{21}X_w + m_{22}Y_w + m_{23}Z_w + m_{24} - m_{31}Y_f X_w - m_{32}Y_f Y_w - m_{33}Y_f Z_w = m_{34}Y_f \end{cases} \quad (2)$$

Theoretically, parameters from m_{11} to m_{34} can be determined by six points. However, in practical applications, m_{34} is always treated as one, and dozens of calibration points are introduced to reduce the error by solving over-

determined equations. So when the number of the points is N , $2N$ equations can be obtained and expressed as follows, and the matrix M can be calculated from a least-squares procedure.

$$Ax = B,$$

$$A = \begin{bmatrix} X_{w_i} & Y_{w_i} & Z_{w_i} & 1 & 0 & 0 & 0 & 0 & -X_{f_i}X_{w_i} & -X_{f_i}Y_{w_i} & -X_{f_i}Z_{w_i} \\ 0 & 0 & 0 & 0 & X_{w_i} & Y_{w_i} & Z_{w_i} & 1 & -Y_{f_i}X_{w_i} & -Y_{f_i}Y_{w_i} & -Y_{f_i}Z_{w_i} \end{bmatrix}, \quad (3)$$

$$X = [m_{11} \ m_{12} \ m_{13} \ m_{14} \ m_{21} \ m_{22} \ m_{23} \ m_{24} \ m_{31} \ m_{32} \ m_{33}]^T,$$

$$B = \begin{bmatrix} X_{f_i} \\ Y_{f_i} \end{bmatrix} \quad i = 1, 2, 3 \dots N.$$

We do not take into consideration the distortion of the lens and other nonlinear factors during this discussion, and a calibration technique simply based on this method will cause much error. So another method is proposed, which divides the whole image area into several parts, and this also means the data pairs (space point coordinates and their corresponding pixel coordinates) are divided into several sets. The linear method mentioned will be applied to each set of data pairs or image regions, respectively. Several transformation matrices will be calculated from this method and when measurement is needed, each of the matrices will be used to input datasets based on the classification rules of the region division. This technique not only improves the calibration precision significantly, but also reduces the number of calibration points for each partition, which simplifies the design of the target. This is the basic concept of the linear partition method.

2.5 Data Integration for Multisensors at Superposition Areas

Because the visual field of a single sensor is limited, several sensors are always needed to see the whole object. An area on the object seen by both sensors is called the superposition area. After the measurement process, both of the two sensors will create datasets at the superposition area, therefore, datasets belonging to the superposition area should be integrated to eliminate redundancy. It is a key part of the preprocess of the scanning data, otherwise two curves will appear at the superposition area. As was mentioned before, the precision of the calibration points, the methods for image capturing and processing, the selection of the calibration technique, and other factors relating to calibration and measurement processes are identical to each of the sensors. Therefore, averaging the superposition data would be simple but efficient. An average coordinates

method is proposed to calculate the datasets at the superposition area, which can be classified into two cases as shown in Figs. 3 and 4.

Figure 3 is a case of data integration of two adjacent sensors. Curves $S1$ and $S2$ are the dataset obtained by two sensors, respectively. The number and the coordinates of the points on each curve at the superposition area are different due to the tiny differences in the sample and calibration process. The data integration process can be performed in the following steps.

Step 1: Select one endpoint on curve $S1$, such as $A1$, and find the closest point on curve $S2$; $A2$ will be found. Then select another endpoint $B1$ on curve $S1$ and find the closest point on curve $S2$; $C2$ will be found.

Step 2: Select one endpoint on curve $S2$, such as $A2$, and find the closest point on curve $S1$; $C1$ will be found. Then select another endpoint $B2$ on curve $S2$ and find the closest

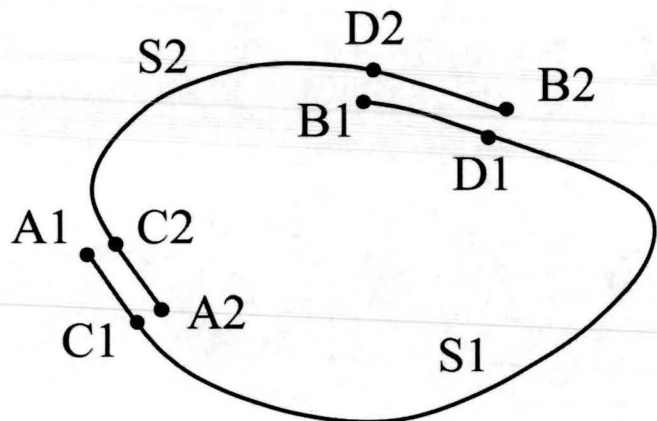


Fig. 4 Data integration of all sensors.

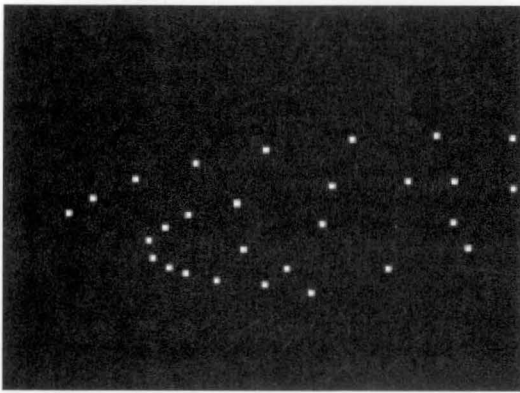


Fig. 5 Calibration image captured by sensor 1.

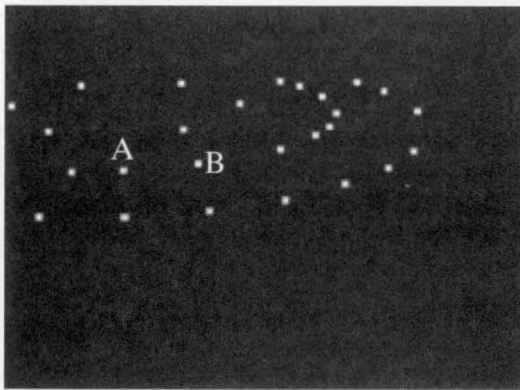


Fig. 6 Calibration image captured by sensor 2.

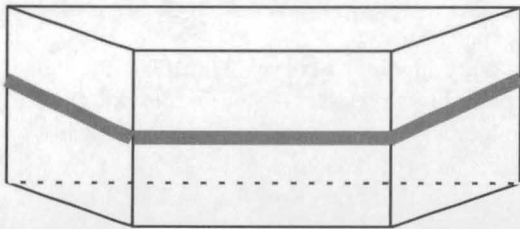


Fig. 7 Model of the object with a certain edge.

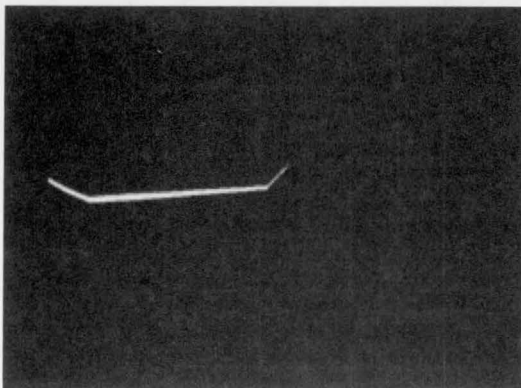


Fig. 8 Object image captured by a single sensor.

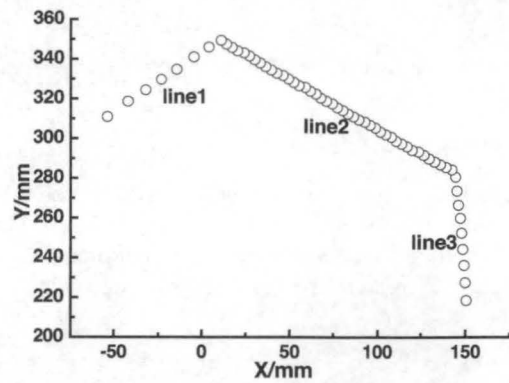


Fig. 9 Measuring result of the edge by a single sensor.

point on curve S_1 ; B_1 will be found. Therefore, the superposition data can be defined as the points between C_1 and B_1 on curve S_1 and points between A_2 and C_2 on curve S_2 .

Step 3: Select one of the curves A_2 to C_2 and C_1 to B_1 that has fewer points as a base curve. For each point $M(X_n, Y_n)$ on the base curve, find the closest point $M'(X_0, Y_0)$ on the other curve and replace point M with the coordinates defined as follows:

$$X_{\text{new}} = (X_n + X_0)/2, \quad Y_{\text{new}} = (Y_n + Y_0)/2. \quad (4)$$

A new curve S_{new} will be obtained until all of the points on the base curve are processed.

Step 4: Connect the remaining part A_1 to C_1 of curve S_1 , curve S_{new} , and the remaining part C_2 to B_2 of curve S_2 into a new curve.

Data of neighboring sensors can be integrated one by one through the four steps mentioned. For the last sensor, it will turn into the case of Fig. 4. Two superposition parts will appear, and the basic principle of integration is the same as in the previous case, which means finding the closest point for each endpoint of the two curves and defining the superposition parts, then using steps 3 and 4 for each part. A curve without redundancy will be obtained.

All of the techniques and methods mentioned are used to get the contour data of the object at a certain vertical position. Sensors can be synchronously moved vertically to scan the whole object, and calculation can be done in each vertical position to get the entire 3-D information of the object.

3 Experimental Results

Based on the data registration and integration principle, two 3-D sensors, a round filament target, and object with a certain edge length are used to verify the principle. The black and white camera with a 6-mm lens is MTV-0360, made by the Mintron Company, and sampled by an image capture board with a resolution of 640×480 . The laser is SNF-501L670 from the Lasiris Company in Canada. The light is line structured and the wavelength is 670 nm.

Figures 5 and 6 show the calibration images captured by two cameras. Both of the images are partitioned by the form of 1×4 at the area where most of the points distribute and four transformation matrices are obtained for each sen-

Table 1 Measuring results of the edge by two sensors, respectively. Units are in millimeters.

Number Position	Sensor 1			Sensor 2		
	1	2	3	1	2	3
Measure	152.0	152.8	152.2	150.9	150.9	150.4
Order	152.4	152.5	152.2	150.6	150.7	150.4
	152.5	152.7	152.7	150.6	150.2	150.2
Average	152.3	152.7	152.4	150.7	150.6	150.3
Relative error	0.73%	0.99%	0.79%	0.33%	0.40%	0.60%
Mean error		0.84%			0.44%	

sor after the calibration process with the linear partition method. The operation time of computing the matrices for each sensor is about 0.06 s. The coordinates of the light points on the image are extracted by a method with sub-pixel precision, as shown in Eq. (5).

$$x = \frac{\sum_i u_i c_i}{\sum_i c_i}, \quad y = \frac{\sum_i v_i c_i}{\sum_i c_i}, \quad (5)$$

where x and y are the coordinates of the point, u and v are the coordinates of each pixel in the small neighborhood of the point, and c is the grayscale value of the pixel. In addition, from the calibration process mentioned before, it can be seen that the resolution of the horizontal plane in our measurement depends on the relative position of the target to the sensor. The resolution is the real size that a pixel on the image stands for. For example, two points A and B on Fig. 6 are selected and the real distance between them can be calculated and their pixel distance on the image can be achieved through their pixel coordinates also. The quotient of these two distances is the resolution. In this case, the resolution is about 0.8 mm.

To verify the calibration precision, an object with certain edge length 151.2 mm is measured according to the calibration results. Figure 7 shows the model of the object. The bold line on the object is the intersection of the light plane and the object's surface. Figure 8 shows the image captured by a single sensor. For each sensor, the object is placed at three different positions and measured three times for each position. It takes about 0.04 s to calculate the space coordinates of the edge. Figure 9 shows one of the results; there

are three lines in the figure and line 2 is the edge. The discrete data points can be fitted into three lines, and two intersection points can be obtained. The distance between these two points is treated as the length of the edge. Table 1 shows the results and the relative error is less than 1%, which indicates that the proposed calibration technique has relatively high precision.

Another object with edge length 241.0 mm is measured to verify the data registration and integration methods. Each sensor will measure part of the edge and the data will be registered, integrated, and fitted into three lines according to the theory mentioned. Similarly, the object is placed at three different positions and measured three times for each position. It takes about 0.1 s to perform the data registration and integration process, and an edge without redundancy is finally obtained. Figure 10 shows one of the results. There are three different shapes in the figure, and each of them stands for a dataset removing the superposition part of sensor 1, a dataset removing superposition part of sensor 2, and new dataset of the superposition part, respectively. Table 2 shows the detailed results obtained from the two sensors. It indicates that the measurement carried out by the two sensors still has high precision, and the curve shape obtained from the data registration and integration can reflect the object's contour truly, which verifies the feasibility of the theory.

Just as was mentioned in Sec. 2.3, the calibration target is designed for performing a relatively big object measurement. To support this hypothesis, a real human body is digitized and its 3-D point cloud is shown in Fig. 11. The scanning time of the whole body is about 17 s.

4 Conclusion

A linear partition method and average coordinates method are proposed for data registration and integration of 3-D sensors based on a vertical scanning system with a line-structured light source. From the theory analysis and ex-

Table 2 Measuring results of another edge by two sensors together. Units are in millimeters.

	1	2	3	Average	Relative error	Mean error
Position 1	240.1	239.5	239.2	239.6	0.58%	
Position 2	241.6	241.3	241.5	241.5	0.21%	0.28%
Position 3	241.4	241.2	240.7	241.1	0.04%	

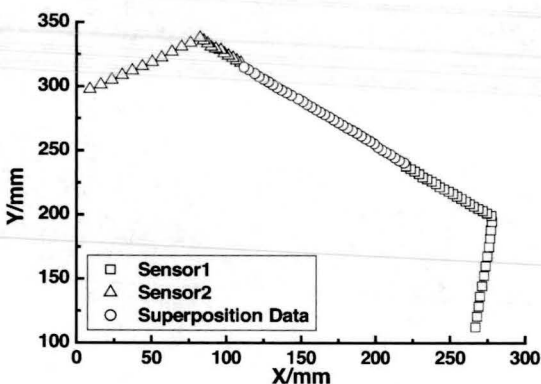


Fig. 10 Measuring result of the edge by double sensors.

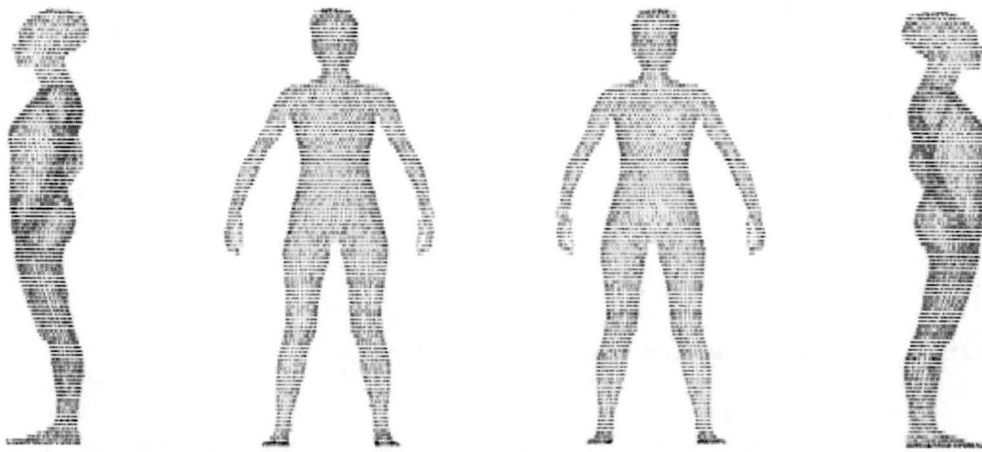


Fig. 11 3-D point cloud of a human body viewed from different sides: (a) left side, (b) front side, (c) back side, and (d) right side.

perimental results given, it indicates that the proposed technique is feasible and can obtain satisfying precision and results. With no requirement for solving nonlinear equations and some basic parameters of the camera, these techniques are easy to adopt, fast running, and are still high in precision, which meets the demands of relatively big object measurement by several sensors. In addition, when the linear partition method is used, the number and form of the partition should be determined by practical application, and the image can be divided by other modes such as concentric circles or rectangles. Furthermore, not only linear but also other nonlinear calibration techniques can be used in each partition, which provides a simple but efficient method for improving current calibration techniques.

Acknowledgments

This work is supported by the National Nature Scientific Research Foundation of China (number 60277009).

References

1. M. Petrov, A. Talapov, T. Robertson, A. Lebedev, A. Zhilyaev, and L. Polonsky, "Optical 3D digitizers: bringing life to the virtual world," *IEEE Comput. Graphics Appl.* **18**(3), 28–37 (1998).
2. J. Forest and J. Salvi, "A review of laser scanning three-dimensional digitizers," *IEEE/RSJ Int. Conf. Intell. Robots System* **1**, 73–78 (2002).
3. G. Baozhen, S. Mingrui, L. Qieni, M. Bing, S. Yuchen, and Z. Yimo, "Research of a laser 3D body scanning system by light stripe method," *J. Optoelectron. Laser* **14**(7), 733–736 (2003).
4. Z. Q. Xu, S. H. Ye and G. Z. Fan, "Color 3D reverse engineering," *J. Mater. Process. Technol.* **129**(1–3), 495–499 (2002).
5. T. Masuda and N. Yokoya, "A robust method for registration and segmentation of multiple range images," *Comput. Vis. Image Underst.* **61**(3), 295–307 (1995).
6. J. Williams and M. Bennamoun, "Simultaneous registration of multiple corresponding point sets," *Comput. Vis. Image Underst.* **81**(1), 117–142 (2001).
7. Z. Guangjun and W. Zhenzhong, "A novel calibration approach to structured light 3D vision inspection," *Opt. Laser Technol.* **34**(5), 373–380 (2002).
8. R. Y. Tsai, "A versatile camera calibration technique for high-accuracy 3D machine vision metrology using off-the-shelf TV cameras and lenses," *IEEE J. Rob. Autom.* **RA-3**(4), 323–344 (1987).
9. M. A. G. Izquierdo, M. T. Sanchez, A. Ibanez and L. G. Ullate, "Sub-pixel measurement of 3D surfaces by laser scanning," *Sens. Actuators, A* **76**(1–3), 1–8 (1999).



Baozhen Ge member of the Chinese Optical Society, received his bachelor, master, and PhD degrees in optical engineering from the College of Precision Instrument and Opto-Electronics Engineering, Tianjin University, China, in 1987, 1990, and 1993, respectively. After postdoctoral research work at the Hong Kong University of Science and Technology from 1999 to 2001, his current research interests include optical electronics information processing, optical instrument, digital holography, and particle measurement.



Yuchen Sun received his bachelor's and master's degrees in optical engineering from the College of Physics Science and Technology, Hebei University, Baoding, China, in 1999 and 2002, respectively. Now he is doing research work at the College of Precision Instruments and Opto-Electronics Engineering, Tianjin University, China. His current research mainly focuses on optical electronics information processing and 3-D laser color digitization.

Biographies and photographs of the other authors not available.